Antiviral Research 240 (2025) 106205

Contents lists available at ScienceDirect

Antiviral Research

journal homepage: www.elsevier.com/locate/antiviral

Identification of pan-flavivirus compounds from drug repurposing

Fatima Zahra Lissane Eddine [a], Gregory Mathez [a], Vincent Carlen [a], Isabela Dolci [b], Rafaela Sachetto Fernandes [b], Andre Schutzer Godoy [b,c], Benoît Laleu [c], Valeria Cagno [a,*]

[a] Institute of Microbiology, University Hospital of Lausanne, University of Lausanne, 1011, Lausanne, Switzerland
[b] São Carlos Institute of Physics, University of São Paulo, Av. João Dagnone, 1100 - Jardim Santa Angelina, São Carlos, 13563-120, Brazil
[c] MMV Medicines for Malaria Venture, ICC, Route de Pré-Bois 20, 1215, Geneva, Switzerland

ARTICLE INFO

Keywords:
Pan-flavivirus
Drug-reporposing
Protein protein interaction
Replication inhibitor

ABSTRACT

The incidence of orthoflavivirus infections is on the rise, yet effective antivirals are unavailable for all members of this family. Additionally, new orthoflaviviruses are emerging, highlighting the need for antiviral strategies with a pan-flavivirus activity. In response, the Global Health Priority Box was screened, leading to the identification of a compound with pan-flavivirus activity. This hit compound demonstrated inhibition of viral replication, consistent efficacy across various cell lines, and maintained activity even at high multiplicity of infection. Importantly it has a high barrier to resistance and possibly acts through a novel mechanism of action. Due to these attributes and its favorable in vitro ADMET profile, compound MMV1791425 emerges as a promising candidate for the future development of a pan-flavivirus antiviral.

1. Introduction

Orthoflaviriruses are genus of the *Flaviviridae* family of RNA viruses that are primarily transmitted by arthropod vectors. In this genus there are multiple important human pathogens such as Dengue virus (DENV), Zika Virus (ZIKV), West Nile Virus (WNV), Yellow Fever Virus (YFV) and Japanese Encephalitis Virus (JEV) transmitted by mosquitoes, and Tick-Borne Encephalitis virus (TBEV) transmitted by ticks. These viruses can cause either visceral or neurological diseases (Pierson and Diamond, 2020) with a wide range of symptoms. Globally they cause a high number of infections, morbidity, and mortality. For instance, the World Health Organization (WHO) estimates that yellow fever virus (YFV) alone causes between 29,000 and 60,000 deaths annually in Africa (2025). Additionally, in 2023, 6.5 million infections were reported as related to DENV (WHO, 2025) and the partial counts for 2024 are at 13 million infections. Climate change and globalization are further accelerating the spread of the vectors and diseases. For instance, in recent years autochthonous transmission of DENV was recorded in Europe (Carletti et al., 2024), underlying the need for preventive and therapeutic measures.

Vaccines are available for YFV, JEV and TBEV while a DENV vaccine has been recently approved after showing to be well tolerated and effective in clinical trials (Tricou et al., 2024). In contrast, no antiviral is available for these viruses, but some promising compounds are currently under development (Palanichamy Kala et al., 2023). Interestingly the DENV inhibitor JNJ1802 (Kesteleyn et al., 2024) and its precursors (Goethals et al., 2023) and YFV inhibitors BDAA (Gao et al., 2022; Guo et al., 2016) are targeting homologous sites on NS4B disrupting viral replication. Notwithstanding, several inhibitors of the NS5 RNA-dependent RNA polymerase (RdRp) are currently in clinical trials (Feracci et al., 2023; Zhou et al., 2024). However, no pan flavivirus inhibitor is currently in development and previously identified compounds with pan-flavivirus activity such as the adenosine analogue NITD008 (Yin et al., 2009) were halted for development due to toxicity issues.

In this scenario repurposing existing compounds could represent a fast track for drug development, as was largely done during COVID-19 and other viruses (Franzi et al., 2023; Rodrigues et al., 2022). This approach allows to screen compounds previously developed for a different pathology to identify potential hits which can be then further optimized.

In line with this approach, we tested the Global Health Priority Box (Adam et al., 2024) against two medically significant flaviviruses, TBEV and WNV, which are responsible for severe infections and lack available antiviral treatments. We identified two compounds with activity at non-toxic concentrations and subsequently characterized their inhibition spectrum and mechanisms of action. Compound MMV1791425 (hereafter named compound 425) emerged as a potential pan-flavivirus

* Corresponding author. Institute of Microbiology of Lausanne, Rue du Bugnon 48, 1011, Lausanne, Switzerland.
E-mail address: valeria.cagno@chuv.ch (V. Cagno).

https://doi.org/10.1016/j.antiviral.2025.106205
Received 29 November 2024; Received in revised form 28 May 2025; Accepted 30 May 2025
Available online 30 May 2025

inhibitor, demonstrating micromolar to submicromolar inhibitory activity at non-toxic doses against WNV, TBEV, ZIKV, USUV, DENV, JEV and YFV. This inhibition targets a replication step and is maintained even with high viral loads and across different cell systems. Furthermore, its in vitro ADMET (absorption–distribution–metabolism–excretion–toxicity) profile is favorable, presenting the opportunity for further optimization toward preclinical studies.

2. Materials and methods

2.1. Cells and viruses

African green monkey fibroblastoid kidney cells (Vero E6), human hepatoma-derived cells (Huh7), baby hamster kidney cells (BHK-21), lung epithelial cells (A549) and neuroblastoma cells (SH5YSY) were kindly given by the laboratory of Sylvia Rothenberger (University of Lausanne, Lausanne) while HeLa cells were obtained by the laboratory of Caroline Tapparel. Cells were maintained in Dulbecco's Modified Eagle's Medium (DMEM) high glucose + Glutamax (Gibco, ThermoFisher Scientific), supplemented with 10 % heat-inactivated fetal bovine serum (FBS; Pan Biotech) and 1 % penicillin/streptomycin (P/S) 100 UI/ml (Gibco, ThermoFisher Scientific), in 75 cm^2 culture flasks (Sigma Aldrich) at 37 °C in an incubator with 5 % CO_2. The WNV-Rep-Rluc cell line, was generated with the pWNVII-Rep-Ren-IB replicon (strain WNV 956 D117 3B) (Pierson et al., 2006) and maintained in DMEM containing 10 % FBS and 1 % P/S, supplemented with 5 μg/ml of blasticidin (InvivoGen) in 75 cm^2 culture flasks at 37 °C in an incubator with 5 % CO_2. Aedes albopictus C6/36 cells were kindly given by the laboratory of Gilbert Greub (University of Lausanne, Lausanne) and maintained in Minimum Essential Medium (MEM; Gibco, ThermoFisher Scientific), supplemented with 10 % heat-inactivated FBS, 1 % P/S and 1X NonEssential Amino Acids (NEAA; Gibco, ThermoFisher Scientific) in 75 cm^2 culture flasks at 28 °C in an incubator with 5 % CO_2. Cells were plated into 96, 24, or 6-well plates 24 h before the experiments with high glucose DMEM + Glutamax, supplemented with 10 % FBS +1 % P/S.

YFV17D, USUV and JEV strains were propagated in Huh7 cells, DENV in BHK21 cells, TBEV Neudorf strain in A549 cells, RVA16 in HeLa cells, whereas the RSV GFP (Hallak et al., 2000), ZIKV Puerto Rico strain, WNV MB NY99 and HSV-2 in Vero E6 cells in high glucose DMEM + Glutamax supplemented with 2.5 % FBS + 1 % P/S. Upon observing cytotoxicity, supernatants were collected and clarified at 2000 rpm for 10 min, and subsequently stored at −80 °C.

2.2. Virus titrations

Plaque assays were performed to quantify infectious viral titers. Cells were infected with the respective viruses in DMEM supplemented with 2.5 % FBS and incubated for 1 h at 37 °C. Following incubation medium containing 0.5 % methylcellulose in 2.5 % DMEM (for HSV-2, WNV and ZIKV) or 0.4 % Avicel in 2.5 % DMEM (for TBEV, USUV and YFV) was added to the cells. The cells were then incubated for 3 day at 37 °C with 5 % CO_2, then fixed and stained using a crystal violet (Sigma Aldrich) for 20 min at room temperature and washed with PBS. Plaques were counted, and the infectious virus titer was expressed as plaque-forming units (pfu)/mL.

2.3. Compounds

Compounds were obtained from the Global Health Priority Box from MMV (Medicines for Malaria Venture). The library contains 80 compounds with activity against drug-resistant malaria, 80 compounds from a library of Bristol-Myers Squibb for neglected and zoonotic diseases and 80 compounds with activity against various vector species. Compounds were dissolved in dimethyl sulfoxide (DMSO; Sigma Aldrich) at a final concentration of 10 mM and thawed before use in a water bath to ensure compound solubility. They were diluted to their final concentrations in medium supplemented with 2.5 % FBS and 1 % P/S.

WNV IgG positive serum (0325-0062) was purchased from SeraCare, decomplemented at 56 °C for 30 min before testing, centrifuged and the supernatant was stored at −20 °C.

2.4. WNV and TBEV screening of MMV Global Health Priority Box

Huh7 (1×10^5 cells/well) were seeded in 96 well plate. The following day 1 or 5 μM of compounds belonging to the Global Health Priority Box were added on cells for 1h at 37 °C, with TBEV or WNV at MOI 0.01, for 96h or 72h respectively. At the end of the incubation the cells were fixed and subjected to immunostaining as described below. The percentage of infection was calculated by subtracting the value of cells not infected and then dividing the absorbance in the infected and treated well to the mean of the absorbance in infected wells. The percentage of inhibition was calculated by subtracting the value to 100. In parallel a plate treated with compounds at 10 μM but uninfected was subjected to a cell viability assay. The screening plates were validated if the Z' score was above 0.5 (Zhang et al., 1999) (Supplementary Table 1), considering as the positive control the infected untreated wells and as negative control the infected wells treated with ribavirin (50 μg/ml) for TBEV and CD-MUS (50 μg/ml) for WNV(Jones et al., 2020). Compounds showing inhibitory activity at nontoxic concentrations were selected for further analysis.

2.5. Immunostaining

Cells were fixed with methanol and subsequently washed with PBS, and 50 μL of a blocking solution (0.05 % Tween + 1 % BSA, diluted in PBS) was added for 20 min at room temperature. After a wash with a PBS-Tween solution (0.05 % Tween diluted in PBS), the E protein pan-flavivirus (4G2, Abcam) was diluted in the blocking solution (1:1000), and added for 1 h at 37 °C, followed by the secondary antibody (IgG, anti-human, Cell Signaling) (1:3000) for 1 h at 37 °C. Three additional washes were then done with PBS-Tween. Then, 50 μL of 3,3′,5,5′Tetramethylbenzidine (TMB) were added to each well. After 10 min incubation the reaction was stopped by adding 50 μL of 1M hydrochloric acid (HCl), and the absorbance was measured at 450 nm.

2.6. Cell viability assay

Cell viability assays were conducted using the methylthiazoly diphenyl-tetrazolium bromide (MTT; Sigma Aldrich) method. Cells were seeded at a density of 10×10^3 cells in 96-well plates and incubated overnight at 37 °C with 5 % CO_2. The following day cells were treated with serial dilutions of the compounds. The cells were then incubated for 3 days at 37 °C. Following incubation, the cell medium was discarded, cells were washed and incubated with 50 μL of MTT solution (0.5 mg/ml). Cells were further incubated at 37 °C for 3 h. The supernatant was discarded, and 50 μL of DMSO per well was added to lyse the cells. The absorbance of the cells was measured at 570 nm using a spectrophotometer (Biotek Epoch 2). Half-maximal cytotoxic concentration (CC_{50}) values were determined using GraphPad Prism 9 analyzing data from three independent experiments.

2.7. Plaque assays

Huh7 cells were seeded at a density of 1×10^5 cells in 24-well plates, while Vero E6 cells were seeded at a density of 9×10^4 cells, and incubated overnight at 37 °C, 5 % CO_2. Cells were then infected at a multiplicity of infection (MOI) of 0.001 in 200 μL of medium supplemented with 2.5 % FBS, and incubated for 1 h at 37 °C, 5 % CO_2. After the incubation the virus inoculum was removed, and each compound was added at five concentrations achieved through a three-fold serial dilution in medium with 2.5 % FBS +1 % P/S + 0.5 % methylcellulose (Sigma Aldrich). Additionally, a positive control condition, left

untreated, and a negative control condition not infected nor treated, were included. The cells were then incubated for 2.5 days for USUV and YFV and for 3 days for ZIKV, all at 37 °C, 5 % CO_2. Cells were fixed using a crystal violet solution for 20 min at room temperature and washed with PBS. Plaques were counted, and the half-maximal effective concentration EC_{50} values were determined using GraphPad Prism 9.

2.8. Antiviral assays

Cells were seeded at a density of 10×10^3 cells in 96-well plates and incubated overnight at 37 °C, 5 % CO_2. Cells were then infected with WNV, TBEV, JEV and DENV, RVA16 and RSV at a MOI of 0.002 in 100 µL of high glucose DMEM + Glutamax, supplemented with 2.5 % FBS +1 % P/S, and incubated for 1 h at 37 °C, 5 % CO_2 with the exception of RVA16 which was incubated at 33 °C. Virus-containing medium was aspirated, 100 µL of each compound concentration was added in duplicate to the treated conditions, and 100 µL of high glucose DMEM + Glutamax, supplemented with 2.5 % FBS +1 % P/S were added to the untreated and the blank conditions in duplicate. The cells were then incubated for 3 days at 37 °C, 5 % CO_2 except for RVA16 infected cells which were incubated for 48h at 33 °C. Cells were fixed with 50 µL of Methanol +1 % H_2O_2 for 5 min at room temperature and washed with PBS. The level of infection was determined by immunostaining or by direct GFP expression in the case of RSV, and the EC_{50} values were calculated using GraphPad Prism 9 from three independent experiments.

2.9. MOI assays

Vero E6 cells were seeded at a density of 90×10^3 cells in a 24 well-plate and incubated overnight at 37 °C with 5 % CO_2. Cells were infected with ZIKV at a MOI (MOI) of 0.001, 0.01, 0.1 or 1 in 200 µL of high glucose DMEM + GlutaMAX, supplemented with 2.5 % FBS + 1 % P/S, and incubated for 1 h at 37 °C with 5 % CO_2. Serial dilutions of the compounds were added post infection in medium supplemented with 2.5 % FBS. When untreated wells displayed cytopathic effect, cells were mechanically detached using a pipette tip and centrifuged at 11000 rpm for 2 min. The collected supernatants were preserved at −80 °C and titrated in a 96-well plate. The plaques were visually counted under a microscope, and the infectious virus titer was quantified as plaque-forming units (pfu)/mL.

2.10. Time-of-addition assay

Experiments were performed by plaque assay as previously described. For the pre-addition treatment, compounds were incubated with the cells for either 1 h or 3 days at 37 °C, followed by a wash and subsequent infection with ZIKV at a 0.001 MOI for 1 h. In the co-addition protocol, the virus and the compounds were added to the cells simultaneously and washed off after 1 h. For the post-addition assay cells were infected and then treated immediately after the removal of the inoculum or at 2h, 4h, 6h, 16h, or 24h post-infection with 500 µL of compound in medium supplemented with methylcellulose. After three days from the infection, cells were fixed using a crystal violet solution for 20 min at room temperature and washed with PBS. Plaques were counted under the microscope, and the EC_{50} values were determined using GraphPad Prism 9.

2.11. Generation of Vero cells stable cell line

Vero cells were seeded in a 6-well plate at a density of 3×10^5 cells and incubated at 37 °C and 5 % CO_2 the day before the experiment. The cells were transfected with the pWNVII-Rep-Ren-IB replicon (Pierson et al., 2006) (2 µg). After 24 h, the medium was either replaced with a selection medium containing 5 µg/mL of blasticidin. Once the cells reached 80 % confluence, they were transferred to a 10 cm dish for further expansion. Single colonies were isolated either by direct trypsinization or by subsequential dilutions. The cells were closely monitored over the weeks, and only wells containing a single surviving colony were selected for further amplification to establish monoclonal WNV-Rep-Rluc cell lines. Cells were then amplified and preserved in a cryoprotective solution (10 % DMSO and 90 % FBS) in liquid nitrogen for future use.

2.12. Validation of Vero cells stable cell line

The stable cell line clones were validated by measuring the renilla luciferase expression, by immunofluorescence with an antibody specific for the WNV NS5 protein (PA5-111986 ThermoFisher Scientific) or by Western blot. Cell lysates were obtained by adding 200 µl of freshly made RIPA buffer (Tris 50 mM pH 7–8, NaCl 150 mM, 0.1 %SDS, 0.5 % Sodium deoxycholate, 1 % Triton X-100, and Protease Inhibitor) directly to cells in 6-well plates, followed by incubation for 20 min in a cold room with agitation. The lysate was centrifuged, and the supernatant was used for quantification using the BCA method, and subsequently loaded on 8 % acrylamide gels. Following electrophoresis, the proteins were transferred onto nitrocellulose membranes and incubated with an antibody anti NS5 (PA5-111986 ThermoFisher Scientific) diluted in 5 % milk/TTBS and a secondary anti-rabbit IgG conjugated with horseradish Peroxidase (HRP) (Cell signaling) diluted 1:2000 in 5 % milk/TTBS and visualized through chemiluminescence with fusion FX (Vilber).

2.13. Luciferase assay for WNV-Rep-Rluc cell line

Rluc-Blast-Rep Vero cells were seeded at 1×10^4 cells in 1 high glucose DMEM + GlutaMAX, supplemented with 10 % FBS and 5 µg/mL of blasticidin. The next day, serial dilutions of the molecules were added in medium supplemented with 2.5 % FBS and blasticidin. After 48 h, luminescence was measured following the Renilla-Glo® Luciferase Assay System (Promega) manufacturer's protocol and read with a luminometer (TriStar LB 941 by Berthold Technologies and the Mikro-Win, 2000 software).

2.14. RNA extraction and qPCR

RNA from infected cells was isolated using (EZNA total RNA extraction kit) and eluted in 40 µL RNase-free water. During RT-qPCR with the TaqPath-1-Step RT-qPCR Master Mix (ThermoFisher Scientific), the ZIKV NS2a protein was targeted for amplification using primers 5′-CTT GGA GTG CTT GTG ATC-3′ and 5′-CTC CTC CAG TGT TCA TTT-3′ and as probe 5′-6-FAM - AGA AGA GAA TGA CCA CAA AGA TCA -BHQ®-1 3'.

2.15. Sequencing

Viral stocks passaged in presence or absence of compound 425 were lysed with TRK Lysis, and total RNA was extracted with E.Z.N.A total RNA extraction according to the manufacturer's protocol. Reverse transcription was performed with SuperScript II (Thermo Fisher) according to the manufacturer's protocol using random primers. The PCR for sequencing were performed with Kapa2G fast (Sigma) according to the manufacturer protocol, using the primers listed in Supplementary Table 2. Microsynth performed the sequencing.

2.16. Resistance selection

Vero E6 cells were seeded on 6-well plates at a density of 2×10^5 cells and incubated overnight at 37 °C and 5 % CO_2. The following day cells were infected and either left untreated or treated with compound 425 at an initial concentration corresponding to the EC_{50}. When the cells displayed extensive cytopathic effect (three- or four-days post-infection), cells were mechanically detached and centrifuged at 2000 rpm for 5 min. The resultant culture supernatants were stored at −80 °C and

titrated using a plaque assay in a 96-well plate. For subsequent passages, cells were infected with a volume of virus adjusted to the titer obtained from the previous passage's conditions at a 0.05 MOI for 1 h at 37 °C. The concentration of the antiviral compound was doubled if the viral titer was comparable to the untreated condition or kept unchanged.

2.17. NS3 inhibition assay

Compound 425 was evaluated in target-based assays against the Zika virus (ZIKV) NS2B-NS3 protease (Fernandes et al., 2021). The proteolytic activity of the viral enzyme was measured by using the fluorogenic peptide substrate Bz-nKRR-AMC 1. The reaction was performed in white 384-well plates using a reaction buffer containing 20 mM Tris pH 8.5, 10 % glycerol and 0.01 % Triton X-100. NS2B-NS3pro was added at a final concentration of 5 nM and compound was tested at a 2-fold serial dilution starting at 100 μM. After a 15 min-incubation at 37 °C, the substrate was added at a final concentration of 30 μM and reaction was maintained at 37 °C, with fluorescence monitored every 1 min and 30 s for 25 min (excitation of 380 nm and emission of 460 nm). Aprotinin was used as positive control (10 μM) while DMSO was used as a negative control of the reactions.

2.18. Structural modelling

To identify the position of G5177T, we used the Zika structures of NS3 helicase and full length NS5 available at the Protein Data Bank (PDB), respectively deposited under codes 5JWH and 5M2X. To assemble into a complex, atomic coordinates were modelled using the cryo-EM structure of the NS5-NS3-SLA complex from DENV, deposited at PDB under code 8GZQ. Analysis and figures were made using ChimeraX v1.6.1 (Meng et al., 2023).

2.19. Mutagenesis

The attempt to generate the G5177T variant was done following the Infectious Subgenomic Amplicons (ISA) method (Aubry et al., 2014). RNA isolation was performed on virus stock using the EZNA total RNA extraction kit according to the manufacturer's protocol. A first fragment (pCMV-2219 bp) and the fragment containing the mutation G5177T (4920–7917) were synthetized by GenScript. Following RNA isolation RT was performed using SuperScript III (ThermoFisher) and PCR with Q5 high fidelity DNA polymerase (New England Biomed) to generate the two remaining fragments. The PCR products were purified, and the four overlapping fragments were transfected in 293T cells with Lipofectamine 3000 as previously described (Darmuzey et al., 2024).

2.20. Solubility in phosphate buffered saline (PBS) pH 7.4

The solubility assay was performed using a miniaturized shake flask method. A solution of phosphate buffered saline (PBS) and the test compound (200 μM) was incubated at 25 °C with constant shaking (600 rpm) for 2 h. The samples were filtered using a multiscreen solubility filter plate. The filtrate was half diluted in acetonitrile. A five-point linearity curve was prepared in PBS:Acetonitrile (1:1, v/v) at 200, 150, 75, 25 and 2.5 μM. Blank, linearity and test samples (n = 2) were transferred to a UV readable plate and the plate was scanned for absorbance. Best fit calibration curves were constructed using the calibration standards and used to determine the test sample solubility. The experiment was carried out in duplicate. Diethylstilbestrol, haloperidol and sodium diclofenac were used as reference standards.

2.21. LogD pH 7.4

The LogD pH7.4 assay was performed using a miniaturized shake flask method. A solution of a pre-saturated mixture of 1-octanol and PBS (1:1, v/v) and the test compound (75 μM) was incubated at 25 °C with constant shaking (850 rpm) for 2 h with the organic and aqueous phases were separated, and samples of each phase transferred to plate for dilution. The organic phase was diluted to 1000-fold and the aqueous phase was diluted 20-fold. The samples were quantitated using LC-MS/MS. The experiment was carried out in duplicate. Propranolol, amitriptyline and midazolam were used as reference standards.

2.22. Metabolic stability study using human liver microsomes

A solution of the test compounds in PBS (1 μM) was incubated in pooled human liver microsomes (0.5 mg/mL) for 0, 5, 20, 30, 45 and 60 min at 37 °C in the presence and absence of NADPH regeneration system (NRS). The reaction was terminated with the addition of ice-cold acetonitrile containing system suitability standard at designated time points. The sample was centrifuged (4200 rpm) for 20 min at 20 °C and the supernatant was half diluted in water and then analyzed by means of LC-MS/MS. % Parent compound remaining, half-life (T1/2) and clearance (CLint,app) were calculated using standard methodology. The experiment was carried out in duplicate. Verapamil, diltiazem, phenacetin and imipramine were used as reference standards.

2.23. Metabolic stability using cryopreserved human hepatocytes

A solution of the test compound in Krebs-Henseleit buffer solution (1 μM) was incubated in pooled human hepatocytes (1×10^6 cells/mL) for 0, 15, 30, 45, 60, 75 and 90 min at 37 °C (5 % CO_2, 95 % relative humidity). The reaction was terminated with the addition of ice-cold acetonitrile containing system suitability standard at designated time points. The sample was centrifuged (4200 rpm) for 20 min at 20 °C and the supernatant was half diluted in water and then analyzed by means of LC-MS/MS. % Parent compound remaining, half-life (T1/2) and clearance (CLint,app) were calculated using standard methodology. The experiment was carried out in duplicate. Diltiazem, 7-ethoxy coumarin, propranolol and midazolam were used as reference standards.

2.24. Metabolic stability using cryopreserved rat hepatocytes

A solution of the test compound in Krebs-Henseleit buffer solution (1 μM) was incubated in pooled rat hepatocytes (1×10^6 cells/mL) for 0, 15, 30, 45, 60, 75 and 90 min at 37 °C (5 % CO_2, 95 % relative humidity). The reaction was terminated with the addition of ice-cold acetonitrile containing system suitability standard at designated time points. The sample was centrifuged (4200 rpm) for 20 min at 20 °C and the supernatant was half diluted in water and then analyzed by means of LC-MS/MS. % Parent compound remaining, half-life (T1/2) and clearance (CLint,app) were calculated using standard methodology. The experiment was carried out in duplicate. Diltiazem, 7-ethoxy coumarin, propranolol and midazolam were used as reference standards.

2.25. hERG inhibition assay

CHO cells were transferred as suspension in serum-free medium to the QPatch automated patch clamp system and kept in the cell storage tank/stirrer during experiments. All solutions applied to cells including the intracellular solution have been maintained at room temperature (19 °C–30 °C).

The voltage protocol applied during experiments was as follows: outward tail currents were measured upon depolarization of the cell membrane to +20 mV for 2 s (activation of channels) from a holding potential of −80 mV and upon subsequent repolarization to −40 mV for 3 s. A waiting time of 5 s before the next pulse followed. The application protocol consists of five periods, during which vehicle and the test item concentrations were applied with increasing order. The voltage protocol ran at least 20 times in each application period. The tail current amplitudes at the end of each period were used in further evaluation steps.

To achieve an appropriate level of statistical significance the test

item (as specified in 4.8.2) were analyzed in sufficient numbers of cells (at least n = 2). E−4031 was used as reference positive control compound. E−4031 at a concentration of 100 nM, which showed to block effectively the hERG tail current in this study (3.88 ± 1.91 % relative remaining current, mean ± SD of n = 2).

Concentration-response curve was determined and the IC_{50} was calculated using SigmaPlot 11.0. The IC_{50} value and the Hill coefficient were determined by fitting the dose response curve with a 2-parameter logistic function.

2.26. Statistics

Experiments were performed in duplicate and from three to four independent experiments as stated in the figure legends. Results are shown as mean and SEM. The EC_{50} and CC_{50} values for inhibition curves were calculated by regression analysis using the program GraphPad Prism version 9.1 to fit a variable slope sigmoidal dose-response curve.

3. Results and discussion

3.1. Identification of pan-flavivirus inhibitors

The Global Health Priority Box from MMV, containing molecules selected to have activity against pathogens and vectors, was screened against WNV and TBEV on Huh7 cells. The compounds were added at the time of infection and left respectively for 72 or 96h. The plates were then subjected to immunostaining and compounds showing inhibitory activity and reduced toxicity were selected for further analysis (Supplementary Fig. 1), by determining the CC_{50} and EC_{50} in Huh7 cells. Compounds 425 and MMV1794211 hereafter named 211, whose structure is shown in Fig. 1, showed inhibitory activity at nontoxic concentrations (Table 1) and were thus retained for further analysis. Compound 425 was included in the Global Health Priority Box because it was identified as an antimalarial hit with an unknown mechanism of action/resistance. On the other hand, compound 211 belongs to the strobilurin class and was reported to have insecticidal and acaricidal activity (Li et al., 2008).

3.2. Validation of spectrum of inhibition

Since the selected compounds were showing inhibitory activity on two different orthoflaviviruses, additional viruses of medical interest belonging to the genus were selected for testing, namely YFV, USUV, ZIKV, JEV and DENV-2. Additionally, Herpes simplex virus (HSV)-2, Respiratory syncytial virus (RSV), and Rhinovirus (RV) A16 were included as controls to evaluate the specificity of the compounds against a DNA virus, a negative-sense RNA virus, and a positive-sense RNA virus. The tests were run in parallel with the known pan-flavivirus polymerase inhibitor NITD008 as a positive control.

The results, shown in Table 1, demonstrate the pan-flavivirus activity of both compounds, a lack of inhibition against HSV-2, and variable potency against the additional RNA viruses tested. NITD008 behaved as expected, showing inhibitory activity against all orthoflaviviruses and against RVA16 (Shang et al., 2014), while it did not inhibit HSV-2 or RSV.

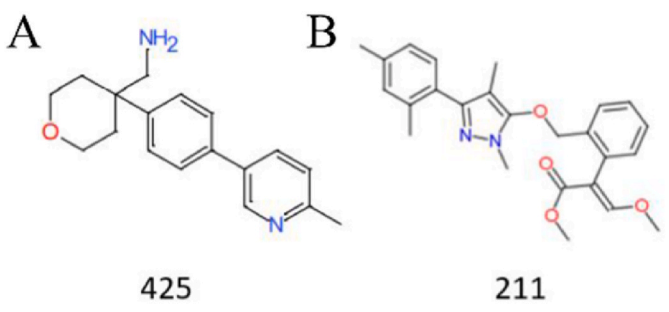

Fig. 1. Structure of the hit compounds.

Table 1
Orthoflavivirus inhibition.

compound	virus	EC_{50} [μM]	95 %CI	CC_{50} [μM]	SI
211	TBEV[a]	0.023	0.021–0.025	6.47	281.3
	WNV[a]	0.018	0.016–0.021	6.47	359.4
	ZIKV[b]	0.05	0.04–0.06	>50	>1000
	USUV[a]	0.1	0.083–0.119	6.47	64.7
	YFV[a]	0.03	0.008–0.055	6.47	215.7
	JEV[a]	0.008	0.007–0.009	6.47	808.8
	DENV-2[a]	0.016	0.011–0.022	6.47	404.4
	HSV-2[b]	>5		>50	
	RSV[b]	0.026	0.011–0.051	>50	>1923
	RVA16[c]	0.27	0.08–2.45	1.23	4.5
425	TBEV[a]	0.89	0.78–1.01	11.59	13.02
	WNV[a]	0.33	0.27–0.41	11.59	35.12
	ZIKV[b]	0.24	0.16–0.34	11.64	48.5
	USUV[a]	0.77	0.59–1.07	11.59	15.05
	YFV[a]	0.62	0.54–073	11.59	18.69
	JEV[a]	0.88	0.77-0.1.00	11.59	13.17
	DENV-2[a]	0.14	0.12–0.17	11.59	82.79
	HSV-2[b]	>5		11.64	
	RSV[b]	1.69	1.41–2.04	11.64	6.89
	RVA16[c]	1.49	0.93–2.36	24.1	16.2
NITD008	TBEV[a]	0.24	0.18–0.32	>50	>208.3
	WNV[a]	0.33	0.19–0.60	>50	>151.5
	ZIKV[b]	0.11	0.09–0.12	>50	>454.5
	USUV[a]	0.25	0.22-0-30	>50	>200
	YFV[a]	0.074	0.049–0.102	>50	>675.7
	JEV[a]	0.37	0.32–0.43	>50	>135.1
	DENV-2[a]	0.24	0.18–0.33	>50	>208.3
	HSV-2[b]	>5		>50	
	RSV[b]	>10		>50	
	RVA16[c]	0.067	0.057–0.078	43.2	644.8

EC_{50}: 50 % effective concentration; CC_{50}: 50 % cytotoxic concentration; SI: selectivity index.
[a] Experiments performed in Huh7 cells.
[b] Experiments performed in VeroE6 cells.
[c] Experiments performed in Hela cells.

Compound 211 exhibited a narrow selectivity index against RVA16 but showed comparable activity against RSV. Compound 425 displayed a narrow selectivity index against RSV and demonstrated activity against RVA16, albeit at higher EC_{50} values compared to orthoflaviviruses. While these results suggest broad activity against RNA viruses, we focused on the most consistent findings within the orthoflavivirus genus to identify the mechanism of action.

3.3. Investigation of the mechanism of action

To determine the mechanism of action of the compounds a stable cell line expressing the non-structural proteins of WNV and luciferase as a reporter was generated with a construct shown in Fig. 2A, and the expression of non-structural proteins of WNV was verified (Supplementary Fig. 2). The compounds and a commercial WNV positive sera, previously shown to neutralize WNV infection (Ackermann-Gaumann et al., 2024) were then added to the stable cell line and luciferase expression was evaluated 48h later. Compounds 211, 425 and the positive control NITD008 showed inhibition of WNV replicon (Fig. 2B) comparable to the one determined against the WT virus (Table 1) in absence of toxicity, while the serum, acting extracellularly, is not reducing the luciferase expression, as expected. Additionally, time of addition experiments were conducted on ZIKV virus by adding the compounds at different times before infection, or during the infection (Fig. 2C and D). While no inhibition was seen for compound 425, compound 211 was showing an EC_{50} of 0.67 μM when added during the infection, losing efficacy if compared to its addition after the removal of the viral inoculum (EC_{50} of 0.054 μM) (Supplementary

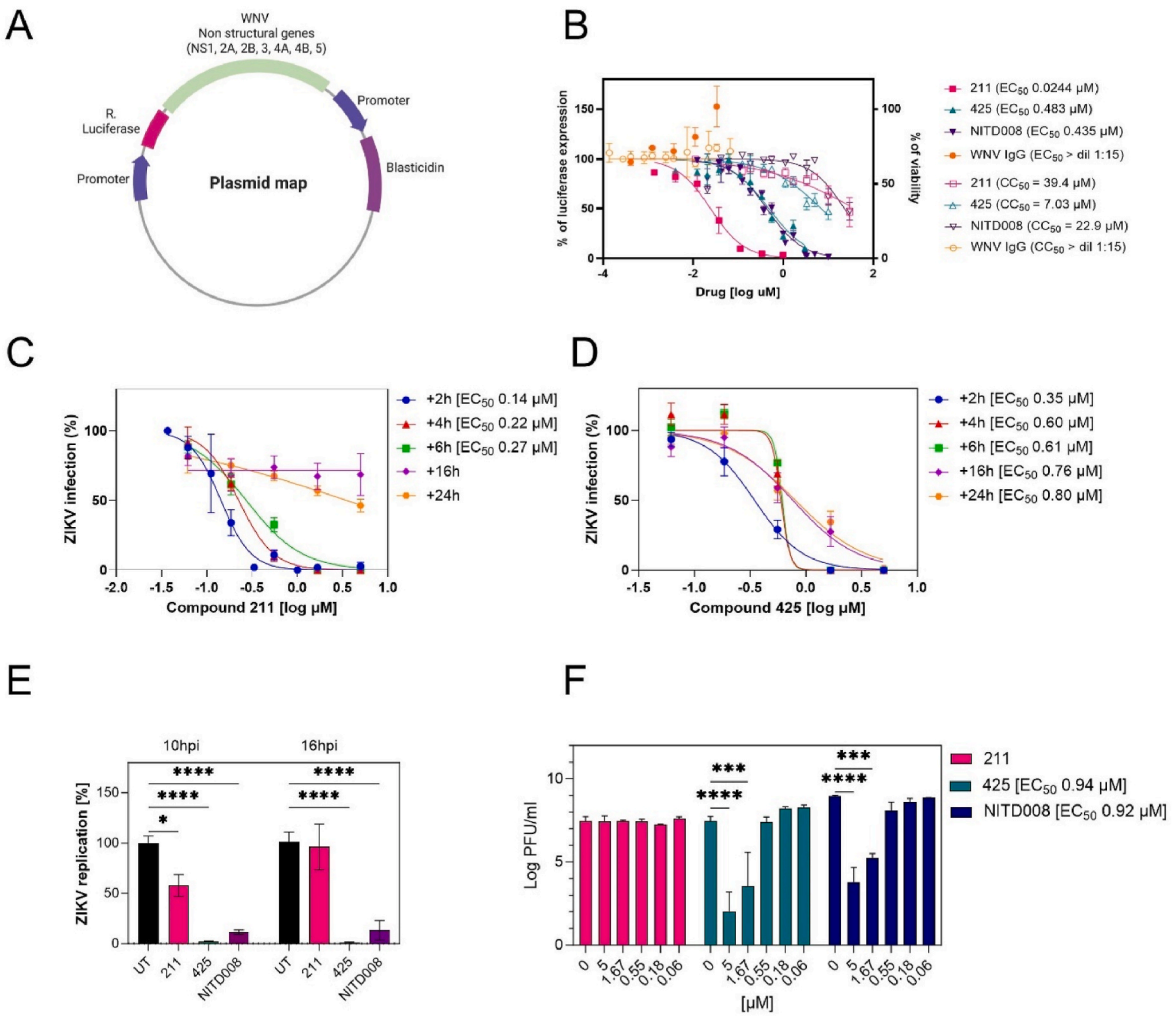

Fig. 2. Mechanism of action of 211 and 425. A) Scheme of the construct used for the generation of WNV replicon stable cell line B) VeroE6 stably expressing the WNV replicon were treated with serial dilution of compounds. Luminescence or viability were evaluated 48h post-treatment. Full symbols represent percentages of luciferase expression, empty symbols percentages of viability. C-D) VeroE6 cells were infected with ZIKV (MOI 0.001) and treated at 2, 4, 6, 16 or 24 h post infection either with compound 211 (C) or with compound 425 (D). Plaques were counted 72hpi. E) VeroE6 cells were infected with ZIKV MOI 1 and immediately after the removal of the viral inoculum with 1.67 µM of the compounds. Cells were lysed at 10 or 16hpi, RNA was extracted and quantified through RT-qPCR. F) Vero E6 cells were infected with ZIKV MOI 1 and treated immediately after the removal of the viral inoculum with serial dilutions of 211, 425 or NITD008. when the untreated wells displayed extensive cytopathic effect supernatants were harvested and titrated. The percentages of infection were calculated by comparing the treated and untreated (UT) wells. EC_{50} and CC_{50} values were calculated with GraphPad Prism. Results are mean and SEM of 3 independent experiments. Two-way Anova was conducted to assess statistical significance *p = 0.0271; ***p < 0.001 ****p < 0.0001.

Fig. 3). In contrast, when the compounds were added at different times post-infection (Fig. 2C and D), the inhibition was maintained if the compounds were added up to 6 hpi. Additionally, compound 425 showed a sustained antiviral activity also when added up to 24 post-infection (Fig. 2D). All together the results show that both 211 and 425 are inhibiting the virus in a post-entry stage, likely at replication and their effect is not linked to egress as shown by the activity on the replicon. To better understand the superior activity of compound 425 despite its higher EC_{50}, if compared with compound 211, additional experiments were performed at MOI 1 by evaluating viral replication through RT-qPCR at 10h, the earliest time point at which viral replication is detected (Supplementary Fig. 4) and at 16h post infection. The results evidenced a high potency of compound 425 both at 10h and 16h, comparable to NITD008, while compound 211 showed significative inhibition only at 10h (Fig. 2E).

Therefore, compound 211, despite showing a low EC_{50} (Table 1) is effective only at low viral concentrations, as was verified as well by a viral yield reduction assay in which it retained activity only at MOI 0.001 and MOI 0.01 (Supplementary Fig. 5). In contrast compound 425 and the control NITD008 were effectively reducing viral yield also at MOI 1 (Fig. 2F) with respective EC_{50}s of 0.94 and 0.92 µM.

3.4. Compound 425 is active on different cell lines

Compound 425 was further tested in more relevant cell lines, namely SH5YSY as representative cells for the neurotropism of ZIKV (Fig. 3A and B) and C6/36, a mosquito cell line (Fig. 3C and D), to evaluate the potential effect of the compound in the vector. In both cellular system the compound retained its inhibitory activity in dose-response assays in absence of toxicity (Fig. 3A–C) and at a single dose at higher MOI (Fig. 3B–D) proving that its activity is not cell-line dependent and is conserved in cell lines mimicking the natural tropism of the virus.

3.5. Compound 425 has a high barrier to resistance and might target the NS3 helicase domain

To evaluate the barrier to resistance of compound 425 and to identify its target, ZIKV was grown in the presence of increasing concentrations

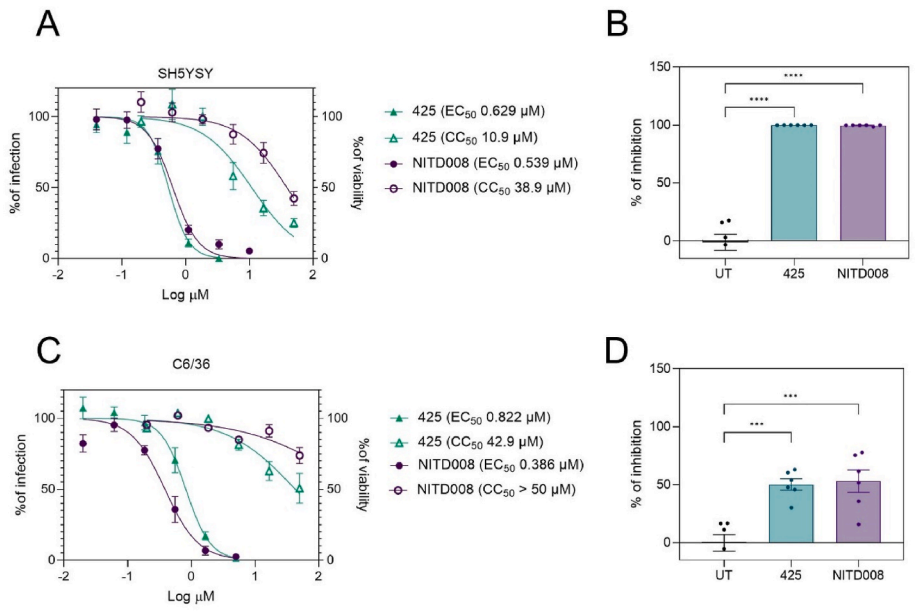

Fig. 3. Breadth of activity of compound 425. Compound 425 and NITD008 were tested in dose-response assays on SHSY5Y (A) and C6/36 cells (C). Cells were either infected with ZIKV at MOI 0.1 or left uninfected, and then treated with compound 425 or NITD008 for 72 h. Infected cells were fixed and subjected to immunostaining, while cell viability in uninfected cells was assessed using an MTT assay. B) SH5YSY or D) C6/36 cells were infected with ZIKV MOI 1 and treated with 1.67 µM of compounds 425 or NITD008 24hpi for SH5YSY or 48hpi for C6/36, RNA was extracted and quantified through RT-qPCR. The percentages of infection were calculated by comparing the treated and untreated (UT) wells. Results are mean and SEM of 3 independent experiments. One-way Anova was conducted to assess statistical significance ***$p < 0.001$ ****$p < 0.0001$. EC_{50} and CC_{50} values were calculated using GraphPad Prism.

of the compound. After 14 passages, the virus cultured with compound 425 showed reduced inhibition compared to previous passages (Fig. 4A) and was subsequently tested in a dose-response assay, revealing a shift in the EC_{50} (Fig. 4B). Whole genome sequencing was then conducted to identify potential mutations responsible for the loss of efficacy. The identified mutations are listed in Fig. 4C.

Given the pan-flavivirus activity of compound 425, conservation of the region of the mutations was assessed. This analysis highlighted that the mutation G5177T, which leads to a substitution at Gln188 within the NS3 helicase domain to a histidine, correspond to the most conserved residue among orthoflaviviruses (Supplementary Fig. 6). This residue is located in the N-terminal portion of the NS3 helicase, positioned opposite to key orthosteric sites such as the RNA-binding cleft and ATP-binding site (Fig. 4D). Notably, recent findings have identified this region as a critical interaction interface with the NS5 RdRp, specifically engaging with its thumb domain (Osawa et al., 2023). Our data suggest that compound 425 may target this interface, potentially inhibiting the assembly of the viral replication complex. A similar mechanism of action, resulting in altered protein-protein interaction, has been observed with JNJ-1802, which blocks the NS3-NS4B interaction and achieves sub-nanomolar potency across all DENV strains (Goethals et al., 2023; Kaptein et al., 2021).

Since the mutation is positioned at the N terminal of the helicase, close to the linker with the protease domain of NS3, a direct activity on the protease was assessed. Compound 425 was tested in a specific assay against NS2B-NS3 protease, showing no inhibition at any of the tested

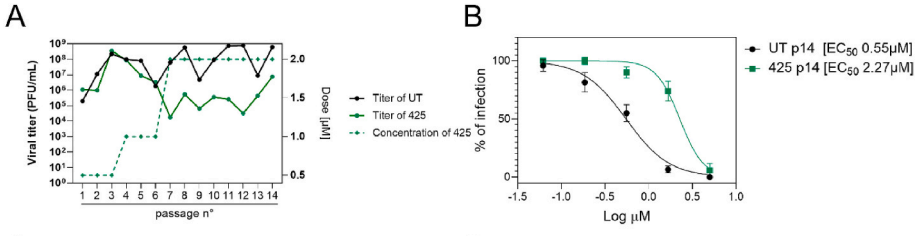

C

PROTEIN	NUCLEOTIDE	AMINOACID CHANGE
NS1	U3038C	silent
NS1	A3282G	K to E
NS3	G5177T*	Q to H
NS3	A5930G*	silent
NS4A	A6519G	R to G
NS4A	A6686G*	silent
2K	A6875G*	I to V
NS5	G8366A	silent

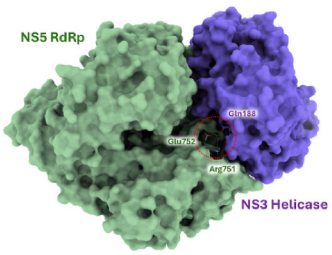

Fig. 4. Resistance selection of compound 425. A) ZIKV was passaged for 14 times in presence or absence of increasing concentrations of compound 425, after each passage the treated and untreated viruses were titered. B) After 14 passages the viruses were tested for their susceptibility to 425 by plaque assay. Results are mean and SEM of three independent experiments. C) The list of mutations identified is shown. Positions are numbered according to sequence NC_035889. *Indicates mixed populations. D) The mutation in the N terminal of the NS3 helicase domain at the interface with NS5 RdRp is highlighted in the red circle.

Table 2
In vitro ADMET characterization of 425.

CL h-LM[a] (µL/min/mg protein)	CL h-Heps[b] (µL/min/10^6 cells)	CL r-Heps[c] (µL/min/10^6 cells)	Caco-2 Papp[d] (efflux ratio) (10^{-6} cm/s)	Solubility[e] (µg/mL)	LogD[f]	hERG IC_{50}[e] (µM)
92.4	20.1	12.2	10.9 (1.7)	199.6	0.61	77.7

g QPatch automated patch clamp (CHO cells).
[a] Intrinsic clearance in human liver microsomes.
[b] Intrinsic clearance in human hepatocytes.
[c] Intrinsic clearance in rat hepactocytes.
[d] Caco-2 cell permeability assay. Papp, permeability coefficient in the apical to basolateral direction.
[e] Aqueous kinetic solubility measured in PBS at pH = 7.4.
[f] Measured LogD at pH 7.4 (shake flask).

doses (Supplementary Fig. 7). Unfortunately, the main limitation of our study is the lack of verification that the introduced mutation reduces viral inhibition, as our attempts to generate mutants using the infectious subgenomic amplicon method (Aubry et al., 2014) failed to produce infectious virus.

3.6. Compound 425 has a favorable ADMET

A preliminary in vitro ADMET of compound 425 was evaluated (Table 2). First, rat and human metabolic stability data were collected. Intrinsic clearance revealed to be in the medium-high range both for microsomes and hepatocytes. As expected, based on the LogD (0.61) and the presence of a basic amine, aqueous solubility is high at pH = 7.4. Despite the modest LogD, a relatively good permeability was observed in Caco-2 cells without significant efflux. Finally, compound 425 exhibit low probability to generate QT prolongation based on lack of inhibition of hERG (human-ether-a-go-go related gene) at concentrations likely to be relevant in vivo studies.

In summary, despite relatively poor metabolic stability that can be explained by the presence of potential metabolic soft spots, compound 425 demonstrated some encouraging in vitro ADMET properties with good permeability and solubility with low risk of hERG.

4. Conclusion

Through the screening of a library of compounds we identified a promising lead, compound 425 showing micromolar to submicromolar activity against multiple orthoflaviviruses at nontoxic concentrations. Despite a higher EC_{50} compared to other flavivirus inhibitors currently in development, such as JNJ1802 (Kesteleyn et al., 2024) or BDAA (Guo et al., 2016), it is important to highlight that this compound, unlike its counterparts, exhibits broader inhibitory activity and has not yet undergone a medicinal chemistry campaign to optimize its potency. Compound 425 retained inhibitory activity when added up to 24 hpi, in multiple cell lines and at MOI 1. The study of the mechanism of action evidenced that the compound is active in a replicative step which is not including entry or egress. The barrier to resistance is high. However, it was possible to select mutants of the virus with a higher EC_{50}. Several mutations were identified, with the most conserved among flaviviruses being in the N terminal of the NS3 helicase domain. This residue is conserved among orthoflavivirus and it is positioned at the interface with the NS5 RdRp suggesting the identification of an inhibitor with a novel mechanism of action. Additionally, we have shown a favorable ADMET profile, despite of modest metabolic stability. Further medicinal chemistry efforts are therefore needed to optimize the antiviral activity and the stability of the compound. In conclusion, the identification of compound 425 could pave the way for developing a new class of pan-flavivirus inhibitors.

CRediT authorship contribution statement

Fatima Zahra Lissane Eddine: Visualization, Methodology, Investigation. **Gregory Mathez:** Visualization, Investigation. **Vincent Carlen:** Investigation. **Isabela Dolci:** Investigation. **Rafaela Sachetto Fernandes:** Supervision, Investigation. **Andre Schutzer Godoy:** Writing – review & editing, Visualization, Investigation. **Benoît Laleu:** Writing – review & editing, Investigation. **Valeria Cagno:** Writing – original draft, Visualization, Supervision, Project administration, Methodology, Investigation, Funding acquisition, Data curation, Conceptualization.

Declaration of generative AI and AI-assisted technologies in the writing process

During the preparation of this work the author(s) used ChatGPT in order to revise the grammar. After using this tool/service, the author(s) reviewed and edited the content as needed and take(s) full responsibility for the content of the publication.

Declaration of competing interest

The authors declare the following financial interests/personal relationships which may be considered as potential competing interests:BL is an employee of MMV. ASG consults for MMV. All other authors declare no conflict of interest.

Acknowledgments

The authors acknowledge MMV, Bristol-Myers Squibb Company and Innovative Vector Control Consortium (IVCC) for support, designing and supplying the Global Health Priority Box. VC acknowledges funding (salary) from SNSF, grant number PZ00P3_193289.

Appendix A. Supplementary data

Supplementary data to this article can be found online at https://doi.org/10.1016/j.antiviral.2025.106205.

Data availability

Data will be made available on request.

References

Ackermann-Gaumann, R., Dentand, A., Lienhard, R., Saeed, M., Speiser, D.E., MacDonald, M.R., Coste, A.T., Cagno, V., 2024. A reporter virus particle seroneutralization assay for tick-borne encephalitis virus overcomes ELISA limitations. J. Med. Virol. 96, e29843. https://doi.org/10.1002/jmv.29843.

Adam, A., Besson, D., Bryant, R., Rees, S., Willis, P.A., Burrows, J.N., Hooft van Huisjduijnen, R., Laleu, B., Norton, L., Canan, S., Hawryluk, N., Robinson, D., Palmer, M., Samby, K.K., 2024. Global Health priority Box horizontal line proactive pandemic preparedness. ACS Infect. Dis. https://doi.org/10.1021/acsinfecdis.4c00700.

Africa, W.R.O.f., 2025. Yellow fever, fact sheet. https://www.afro.who.int/health-topics/yellow-fever.

Aubry, F., Nougairede, A., de Fabritus, L., Querat, G., Gould, E.A., de Lamballerie, X., 2014. Single-stranded positive-sense RNA viruses generated in days using infectious subgenomic amplicons. J. Gen. Virol. 95, 2462–2467. https://doi.org/10.1099/vir.0.068023-0.

Carletti, F., Carli, G., Spezia, P.G., Gruber, C.E.M., Prandi, I.G., Rueca, M., Agresta, A., Specchiarello, E., Fabeni, L., Giovanni, E.S., Arcuri, C., Spaziante, M., Focosi, D., Scognamiglio, P., Barca, A., Nicastri, E., Girardi, E., Chillemi, G., Vairo, F., Maggi, F., 2024. Genetic and structural characterization of dengue virus involved in the 2023 autochthonous outbreaks in central Italy. Emerg. Microb. Infect. 13, 2420734. https://doi.org/10.1080/22221751.2024.2420734.

Darmuzey, M., Touret, F., Slowikowski, E., Gladwyn-Ng, I., Ahuja, K., Sanchez-Felipe, L., de Lamballerie, X., Verfaillie, C., Marques, P.E., Neyts, J., Kaptein, S.J.F., 2024. Epidemic Zika virus strains from the Asian lineage induce an attenuated fetal brain pathogenicity. Nat. Commun. 15, 10870. https://doi.org/10.1038/s41467-024-55155-4.

Feracci, M., Eydoux, C., Fattorini, V., Lo Bello, L., Gauffre, P., Selisko, B., Sutto-Ortiz, P., Shannon, A., Xia, H., Shi, P.Y., Noel, M., Debart, F., Vasseur, J.J., Good, S., Lin, K., Moussa, A., Sommadossi, J.P., Chazot, A., Alvarez, K., Guillemot, J.C., Decroly, E., Ferron, F., Canard, B., 2023. AT-752 targets multiple sites and activities on the Dengue virus replication enzyme NS5. Antivir. Res. 212, 105574. https://doi.org/10.1016/j.antiviral.2023.105574.

Fernandes, R.S., Noske, G.D., Gawriljuk, V.O., de Oliveira, K.I.Z., Godoy, A.S., Mesquita, N., Oliva, G., 2021. High-throughput antiviral assays to screen for inhibitors of Zika virus replication. J. Vis. Exp. https://doi.org/10.3791/62422.

Franzi, E., Mathez, G., Dinant, S., Deloizy, C., Kaiser, L., Tapparel, C., Le Goffic, R., Cagno, V., 2023. Non-steroidal estrogens inhibit influenza virus by interacting with hemagglutinin and preventing viral fusion. Int. J. Mol. Sci. 24. https://doi.org/10.3390/ijms242015382.

Gao, Z., Zhang, X., Zhang, L., Wu, S., Ma, J., Wang, F., Zhou, Y., Dai, X., Bullitt, E., Du, Y., Guo, J.T., Chang, J., 2022. A yellow fever virus NS4B inhibitor not only suppresses viral replication, but also enhances the virus activation of RIG-I-like receptor-mediated innate immune response. PLoS Pathog. 18, e1010271. https://doi.org/10.1371/journal.ppat.1010271.

Goethals, O., Kaptein, S.J.F., Kesteleyn, B., Bonfanti, J.F., Van Wesenbeeck, L., Bardiot, D., Verschoor, E.J., Verstrepen, B.E., Fagrouch, Z., Putnak, J.R., Kiemel, D., Ackaert, O., Straetemans, R., Lachau-Durand, S., Geluykens, P., Crabbe, M., Thys, K., Stoops, B., Lenz, O., Tambuyzer, L., De Meyer, S., Dallmeier, K., McCracken, M.K., Gromowski, G.D., Rutvisuttinunt, W., Jarman, R.G., Karasavvas, N., Touret, F., Querat, G., de Lamballerie, X., Chatel-Chaix, L., Milligan, G.N., Beasley, D.W.C., Bourne, N., Barrett, A.D.T., Marchand, A., Jonckers, T.H.M., Raboisson, P., Simmen, K., Chaltin, P., Bartenschlager, R., Bogers, W.M., Neyts, J., Van Loock, M., 2023. Blocking NS3-NS4B interaction inhibits dengue virus in non-human primates. Nature 615, 678–686. https://doi.org/10.1038/s41586-023-05790-6.

Guo, F., Wu, S., Julander, J., Ma, J., Zhang, X., Kulp, J., Cuconati, A., Block, T.M., Du, Y., Guo, J.T., Chang, J., 2016. A novel benzodiazepine compound inhibits yellow fever virus infection by specifically targeting NS4B protein. J. Virol. 90, 10774–10788. https://doi.org/10.1128/JVI.01253-16.

Hallak, L.K., Collins, P.L., Knudson, W., Peeples, M.E., 2000. Iduronic acid-containing glycosaminoglycans on target cells are required for efficient respiratory syncytial virus infection. Virology (New York, N. Y.) 271, 264–275. https://doi.org/10.1006/viro.2000.0293.

Jones, S.T., Cagno, V., Janecek, M., Ortiz, D., Gasilova, N., Piret, J., Gasbarri, M., Constant, D.A., Han, Y., Vukovic, L., Kral, P., Kaiser, L., Huang, S., Constant, S., Kirkegaard, K., Boivin, G., Stellacci, F., Tapparel, C., 2020. Modified cyclodextrins as broad-spectrum antivirals. Sci. Adv. 6, eaax9318. https://doi.org/10.1126/sciadv.aax9318.

Kaptein, S.J.F., Goethals, O., Kiemel, D., Marchand, A., Kesteleyn, B., Bonfanti, J.F., Bardiot, D., Stoops, B., Jonckers, T.H.M., Dallmeier, K., Geluykens, P., Thys, K., Crabbe, M., Chatel-Chaix, L., Munster, M., Querat, G., Touret, F., de Lamballerie, X., Raboisson, P., Simmen, K., Chaltin, P., Bartenschlager, R., Van Loock, M., Neyts, J., 2021. A pan-serotype dengue virus inhibitor targeting the NS3-NS4B interaction. Nature 598, 504–509. https://doi.org/10.1038/s41586-021-03990-6.

Kesteleyn, B., Bonfanti, J.F., Bardiot, D., De Boeck, B., Goethals, O., Kaptein, S.J.F., Stoops, B., Coesemans, E., Fortin, J., Muller, P., Doublet, F., Carlens, G., Koukni, M., Smets, W., Raboisson, P., Chaltin, P., Simmen, K., Loock, M.V., Neyts, J., Marchand, A., Jonckers, T.H.M., 2024. Discovery of JNJ-1802, a first-in-class pan-serotype dengue virus NS4B inhibitor. J. Med. Chem. 67, 4063–4082. https://doi.org/10.1021/acs.jmedchem.3c02336.

Li, M.L., Ruolin, Yang, Hao, Zhang, Hong, Liu, Changling, Li, Zhengming, 2008. Synthesis and insecticidal and acaricidal activity of (E)-methyl 2-[2-[[3-(2,4-dimethylphenyl)-1,4-dimethyl-1H-pyrazol-5-yloxy]methyl]phenyl]-3-methoxyacrylate (SYP-4903). Nong Yao 47 (12), 874–876.

Meng, E.C., Goddard, T.D., Pettersen, E.F., Couch, G.S., Pearson, Z.J., Morris, J.H., Ferrin, T.E., 2023. UCSF ChimeraX: tools for structure building and analysis. Protein Sci. 32, e4792. https://doi.org/10.1002/pro.4792.

Osawa, T., Aoki, M., Ehara, H., Sekine, S.I., 2023. Structures of dengue virus RNA replicase complexes. Mol. Cell 83, 2781–2791. https://doi.org/10.1016/j.molcel.2023.06.023 e2784.

Palanichamy Kala, M., St John, A.L., Rathore, A.P.S., 2023. Dengue: update on clinically relevant therapeutic strategies and vaccines. Curr. Treat. Options Infect. Dis. 15, 27–52. https://doi.org/10.1007/s40506-023-00263-w.

Pierson, T.C., Diamond, M.S., 2020. The continued threat of emerging flaviviruses. Nat. Microbiol. 5, 796–812. https://doi.org/10.1038/s41564-020-0714-0.

Pierson, T.C., Sanchez, M.D., Puffer, B.A., Ahmed, A.A., Geiss, B.J., Valentine, L.E., Altamura, L.A., Diamond, M.S., Doms, R.W., 2006. A rapid and quantitative assay for measuring antibody-mediated neutralization of West Nile virus infection. Virology (New York, N. Y.) 346, 53–65. https://doi.org/10.1016/j.virol.2005.10.030.

Rodrigues, L., Bento Cunha, R., Vassilevskaia, T., Viveiros, M., Cunha, C., 2022. Drug repurposing for COVID-19: a review and a novel strategy to identify new targets and potential drug candidates. Molecules (Basel) 27. https://doi.org/10.3390/molecules27092723.

Shang, L., Wang, Y., Qing, J., Shu, B., Cao, L., Lou, Z., Gong, P., Sun, Y., Yin, Z., 2014. An adenosine nucleoside analogue NITD008 inhibits EV71 proliferation. Antivir. Res. 112, 47–58. https://doi.org/10.1016/j.antiviral.2014.10.009.

Tricou, V., Yu, D., Reynales, H., Biswal, S., Saez-Llorens, X., Sirivichayakul, C., Lopez, P., Borja-Tabora, C., Bravo, L., Kosalaraksa, P., Vargas, L.M., Alera, M.T., Rivera, L., Watanaveeradej, V., Dietze, R., Fernando, L., Wickramasinghe, V.P., Moreira Jr., E. D., Fernando, A.D., Gunasekera, D., Luz, K., Oliveira, A.L., Tuboi, S., Escudero, I., Hutagalung, Y., Lloyd, E., Rauscher, M., Zent, O., Folschweiller, N., LeFevre, I., Espinoza, F., Wallace, D., 2024. Long-term efficacy and safety of a tetravalent dengue vaccine (TAK-003): 4.5-year results from a phase 3, randomised, double-blind, placebo-controlled trial. Lancet Global Health 12, e257–e270. https://doi.org/10.1016/S2214-109X(23)00522-3.

WHO, 2025. Dengue and severe dengue. https://www.who.int/news-room/fact-sheets/detail/dengue-and-severe-dengue.

Yin, Z., Chen, Y.L., Schul, W., Wang, Q.Y., Gu, F., Duraiswamy, J., Kondreddi, R.R., Niyomrattanakit, P., Lakshminarayana, S.B., Goh, A., Xu, H.Y., Liu, W., Liu, B., Lim, J.Y., Ng, C.Y., Qing, M., Lim, C.C., Yip, A., Wang, G., Chan, W.L., Tan, H.P., Lin, K., Zhang, B., Zou, G., Bernard, K.A., Garrett, C., Beltz, K., Dong, M., Weaver, M., He, H., Pichota, A., Dartois, V., Keller, T.H., Shi, P.Y., 2009. An adenosine nucleoside inhibitor of dengue virus. Proc. Natl. Acad. Sci. U. S. A. 106, 20435–20439. https://doi.org/10.1073/pnas.0907010106.

Zhang, J.H., Chung, T.D., Oldenburg, K.R., 1999. A simple statistical parameter for use in evaluation and validation of high throughput screening assays. J. Biomol. Screen 4, 67–73. https://doi.org/10.1177/108705719900400206.

Zhou, X.J., Lickliter, J., Montrond, M., Ishak, L., Pietropaolo, K., James, D., Belanger, B., Horga, A., Hammond, J., 2024. First-in-human trial evaluating safety and pharmacokinetics of AT-752, a novel nucleotide prodrug with pan-serotype activity against dengue virus. Antimicrob. Agents Chemother. 68, e0161523. https://doi.org/10.1128/aac.01615-23.